united nations educational, scientific and cultural organization

international atomic energy agency

the
abdus salam
international centre for theoretical physics

ICTP 40th Anniversary

SMR 1564 - 24

SPRING COLLEGE ON SCIENCE AT THE NANOSCALE
(24 May - 11 June 2004)

BIOCHIPS - Part II

Rashid BASHIR
School of Electrical & Computer Engineering, Purdue University
West Lafayette, IN, USA

These are preliminary lecture notes, intended only for distribution to participants.

PURDUE UNIVERSITY

Key Topics

- Biochips/Biosensors and Device Fabrication
- Cells, DNA, Proteins
- **Micro-fluidics**
- **Biochip Sensors & Detection Methods**
- Micro-arrays
- Lab-on-a-chip Devices

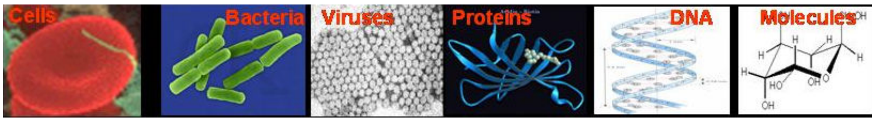

1

PURDUE UNIVERSITY

Continuous Fluid Flows

Navier Stokes Equation (dimensional form)

$$\rho \frac{D\vec{V}}{Dt} = \rho \frac{\partial \vec{V}}{\partial t} + \rho\left(\vec{V} \cdot \nabla\right)\vec{V} = \rho \vec{g} - \nabla p + \mu \nabla^2 V$$

Scale equation:

$$V = uV'; x = Lx'; p = \frac{\mu u}{L} p'; t = \frac{L}{u} t'$$

$$\mathrm{Re}\frac{D\vec{V}}{Dt} = \mathrm{Re}\left(\frac{\partial V}{\partial t} + \left(V \cdot \nabla\right)\vec{V}\right) = \mathrm{Re} \cdot Fr^{-2} \frac{g}{|g|} - \nabla p + \nabla^2 V$$

$$\text{where } \mathrm{Re} = \frac{\rho u L}{\mu}, Fr^{-2} = \frac{gL}{u^2}$$

Wereley, et al. Purdue

2

Dimensionless Parameters

- Assume water flow;

  $\mu=10^{-3}$ kg/(s-m), $\rho=10^{3}$ kg/m^{3}
- Length ~ 10 μm=10^{-5} m
- Velocity ~ 1 mm/s=10^{-3}m/s
- Then: Re=10^{-2}, Fr^{-2}=100,
- N-S equation becomes Poisson Eqn

$$0 = -\nabla p + \nabla^2 V$$

Wereley, et al. Purdue

3

Re in BioChips and Laminar Flow

- **Reynolds number, Re= $LV_{avg}\,\rho/\mu$**
- **Re=inertial forces/viscous forces implies inertia relatively important**
  - ***L*** **is the most relevant length scale,**
  - **μ is the viscosity, ρ is the fluid density,**
  - **V_{avg} is the average velocity of the flow.**
- **Reduced Re**
  - **Higher μ (molasses)**
  - **Reduce flow rate (traffic in Rome!)**
  - **Reduce L (i.e. micro devices)**

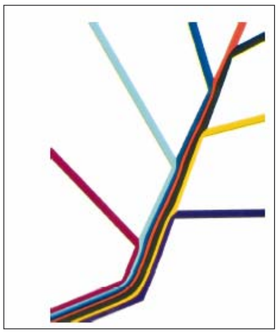

Whitesides et al., (Harvard)

- **Re is usually much less than 100, often less than 1.0 in micro devices**
- **Flow is completely laminar and no turbulence occurs.**

4

Microfluidic Mixing

- Mixing only by diffusion (or novel structures using hydrodynamics)

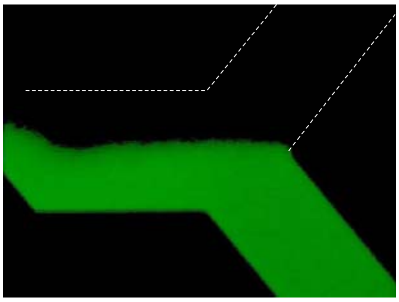

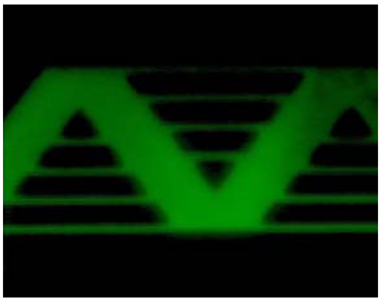

.

Regnier, et al. Purdue

5

Particle Separation

- Particle separation/filter in micro-fluidic devices - without a membrane
- Smaller particles will diffuse farther and will get separated from the flow
- Diffusion distance: $x^2 = 2Dt$ $\quad D = \frac{k_b T}{6\pi\eta a}$
  - biotin (D ~ 350 μm²/s)
  - albumin (D ~ 65 μm²/s)

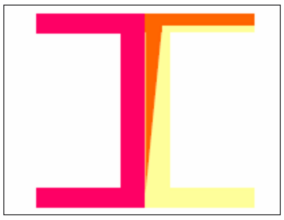

Yager (U. Washington)

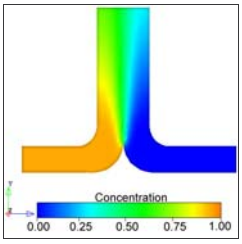

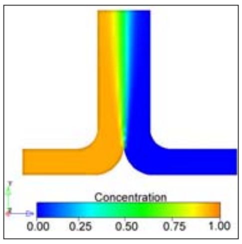

6

PURDUE UNIVERSITY

Microfluidic Flow

- Pressure driven flow
  - Parabolic profile
  - No-slip boundary condition (Velocity at interface is zero)

- Electrokinetic flow
  1. Electroosmosis (EOF)
  2. Electrophoresis (EP)
  3. Dielectrophoresis (DEP)

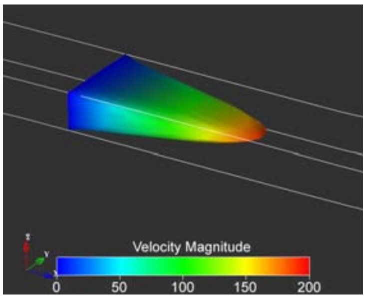

Yager, et al. U. Washington

PURDUE UNIVERSITY

Electroosmotic Flow

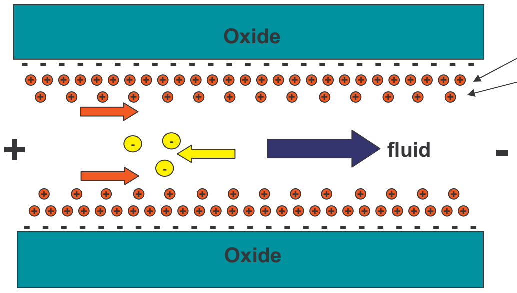

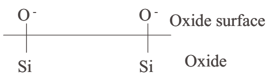

Deprotonation of silanol groups occurs when the pH value of aqueous solution above PZC.

- $Q_{EOF} = \varepsilon\ E\ \zeta\ A/\eta$
  ζ = zeta potential, η = viscosity
- Charges at interface
- Counter ion accumulation at interface
- Results in plug flow
- Electrophoresis also takes place

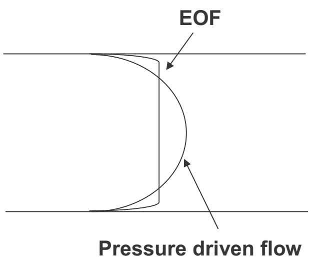

Electroosmotic Flow in Nano-channels

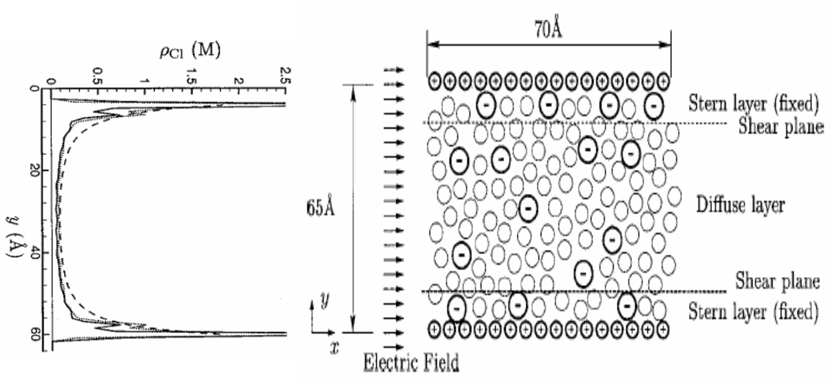

Surface was assumed positively charged. Concentration of Cl ions in bulk is 0.01 M. Concentrations near surface and at middle of channel are 3.21 M and 0.2 M, respectively. ———simulation with uniformly charged wall atoms; ------ simulation with discrete wall atom charges. From *Freund 2002*.

9

Electrophoresis

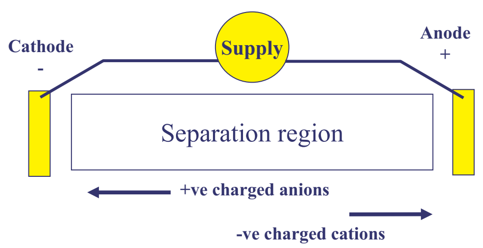

- Electrophoresis: charged species drift when placed under an electric field
- $v = -\mu\, dV/dx$
  - v - electrophoretic velocity
  - μ - electrophoretic mobility
  - dV/dx = applied electric field

10

DNA Gel Electrophoresis

- DNA has phosphate backbone which is negatively charged - hence DNA drifts in an E-field
- The charge/mass (e/m) ratio is constant hence electrophoretic mobility is independent of size in liquid medium.
- Thus, another sieving medium is needed where separation can take place due to difference in length.
- The separation region is filled with a gel - sieving matrix with pores through which the DNA molecules can traverse.
- The field stretches the molecules and they move in a snake-like fashion through the pores of the gel.
- μ in gels is inversely proportional to log of fragment size (sieving effect)
- Polyacrylamide gel is used to separate DNA molecules of 10-500 bases - pores are small
- Agarose gel is used to separate larger molecules (300-10,000 base pairs)

11

DNA Electrophoresis

- Separation $\Delta L = \Delta\mu\, E\, t$
- Resolution of separation is measured by planes N,
  - N = (# of distinguishable bands within the length of the gel)^2
  - N= $\mu V/2D$
    - D is the diffusion coefficient

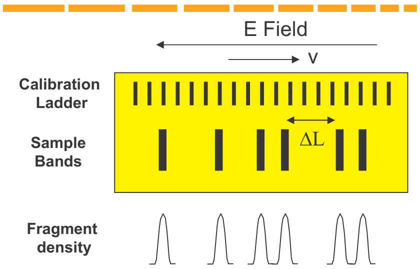

- Higher voltages increase resolution but Joule heating is an issue and needs to be considered
- Separation can also be done in capillaries since higher fields can be used (higher velocities and shorter times)

12

PURDUE UNIVERSITY

DNA Electrophoresis

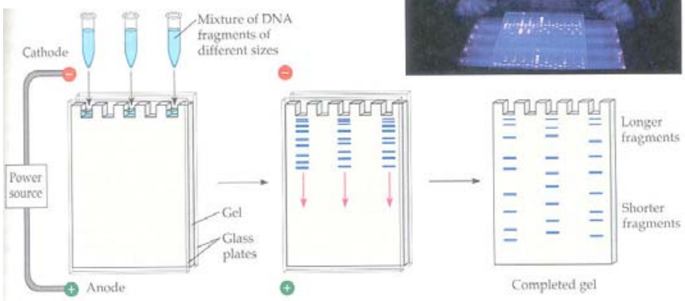

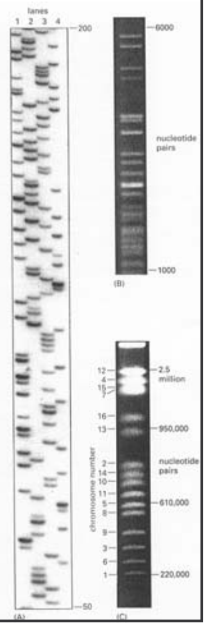

PURDUE UNIVERSITY

DNA Electrophoresis in a Chip

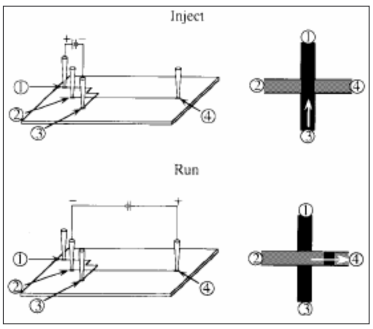

Methias, UCB

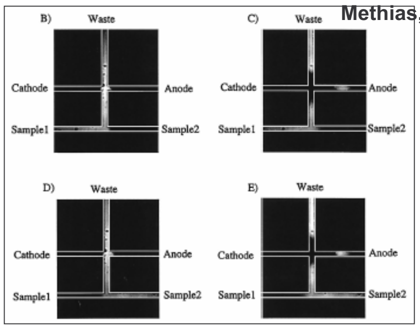

- Small sample size
- Higher fields, higher velocities
- Faster results

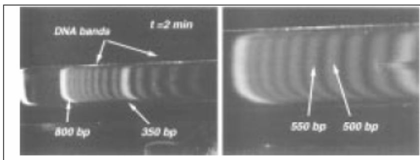

Fig. 22. Injection and separation of DNA fragments on integrated device. The channel is 500 × 50 μm^2 (50 bp ladder, 0.13 $\mu g/\mu L$, SYBR Green, 8 V/cm, 10%T : 2.6%C polyacrylamide) [136].

Mastrangelo, Burns, Univ. of Michigan

14

Dielectrophoresis

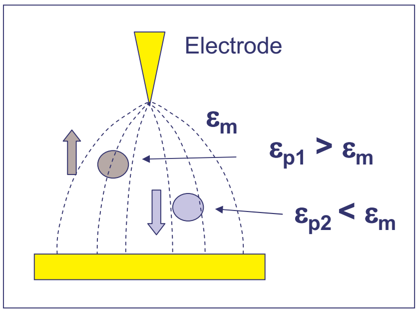

Simplest approximation:

$$F = 2\pi\varepsilon_0\varepsilon_m r^3 \,\mathrm{Re}[f_{CM}]\nabla|E_{RMS}|^2$$

$$f_{CM}(\varepsilon_p,\varepsilon_m) = \frac{\varepsilon_p - \varepsilon_m}{\varepsilon_p + 2\varepsilon_m} \qquad \varepsilon_p = \varepsilon(\omega)$$

15

Dielectrophoresis on Interdigitated Electrodes

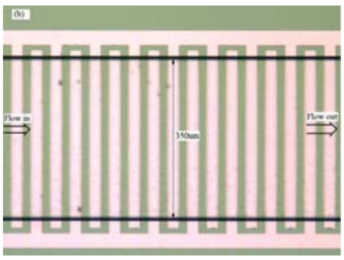

Interdigitated electrodes on a chip

Polystyrene beads : $\varepsilon_p < \varepsilon_m$ → negative DEP

Cells : $\varepsilon_p < \varepsilon_m$ → Negative DEP
Cells : $\varepsilon_p > \varepsilon_m$ → Positive DEP

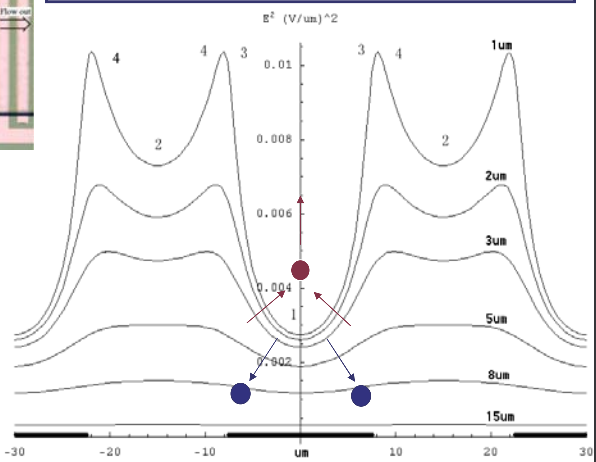

H. Li and R. Bashir, Sensors and Actuators, 2002, JMEMS, 2004

A Dielectrophoretic Filter

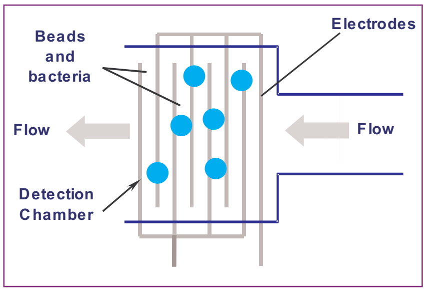

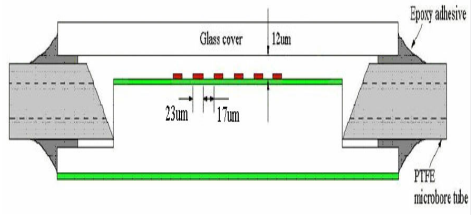

Schematic of the device cross-section

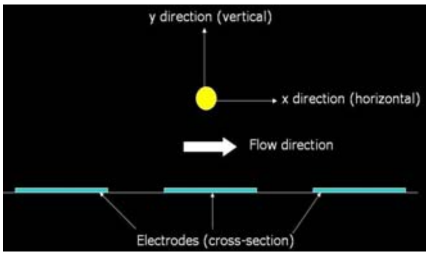

X-component of DEP force at different heights

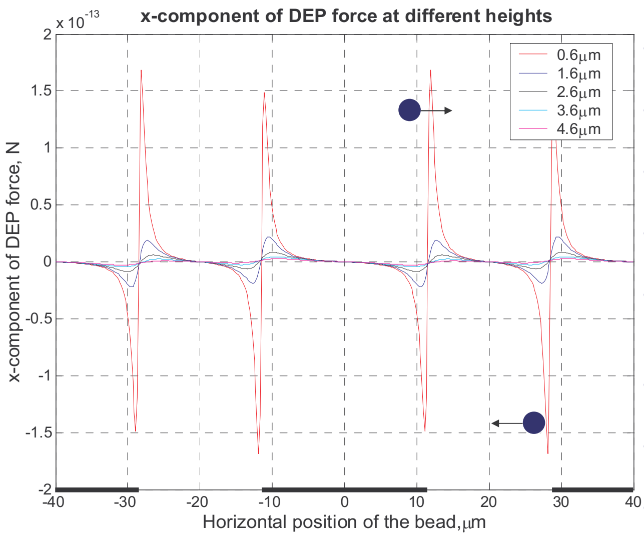

- Bead diameter: 0.7μm
- Bead conductivity: 2e-4 S/m
- Relative permittivity of bead: 2.6
- Bead density: 1.05 g/cm3
- Medium (DI water) conductivity: 2.5 S/m
- Relative permittivity of medium: 80
- Medium density: 1.0 g/cm3
- Voltage: 1Vrms
- Frequency: 580KHz

PURDUE UNIVERSITY

Y-component of DEP force at different heights

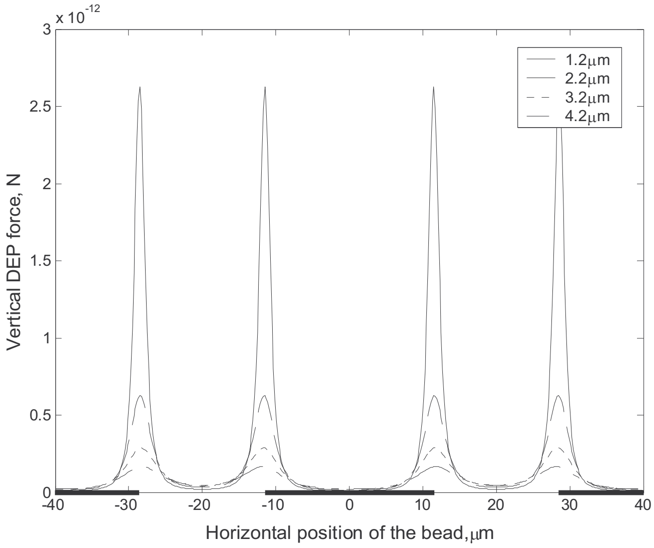

19

PURDUE UNIVERSITY

Forces on a particle in a micro-fluidic flow

- **1. DEP Force**
- **2. Sedimentation Force**

$$F_{sedi} = \frac{4}{3}\pi R^3(\rho_p - \rho_m)g$$

- **3. Hydrodynamic Drag Force:**

$$F_{HD-drag} \approx 6\pi k R \eta(\upsilon_m - \upsilon_p)$$

- **Assume a parabolic laminar flow profile:**

$$\upsilon = 6\langle\upsilon\rangle\frac{x}{h}\left(1-\frac{x}{h}\right) \qquad \langle\upsilon\rangle = \frac{U}{wh}$$

U: flow rate in μl/min

- **4. Hydrodynamic lifting force**

$$F_{HD-lift} \approx 0.153R^2\eta\frac{1}{(x-R)}\cdot\left.\frac{d\upsilon_m}{dx}\right|_{x=0}$$

- **Two orders of magnitude smaller than typical DEP lifting force**
- **Neglected here**

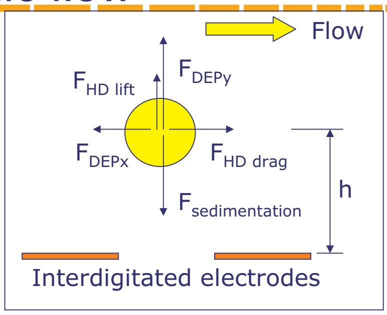

20

PURDUE UNIVERSITY

Trapping of beads (- DEP) and microorganisms (+ DEP)

Holding voltage of the negative DEP traps on interdigitated electrodes versus flow rate for polystyrene beads with different diameters in DI water (conductivity ~1.5μS/cm) at 1MHz

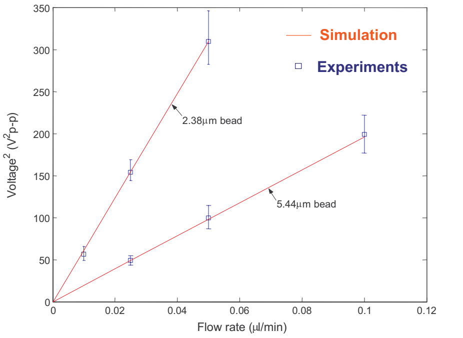

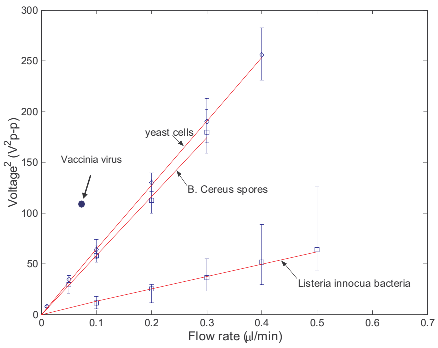

H. Li, Y. Zheng, D. Akin, R. Bashir, submitted to IEEE/ASME JMEMS

21

PURDUE UNIVERSITY

Dielectrophoretic Trapping of *Vaccinia* virus (positive DEP)

- Fluorescent imaging of nano-scale virus particles (Vaccinia virus and Human Corona Virus)
- Trapping of viruses in DEP filters
- Dual labeling of viruses with fluorescent dyes

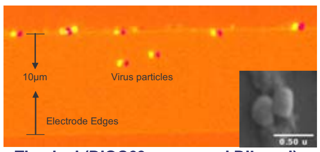

The dual (DiOC63, green and DiL, red) labelled viral particles

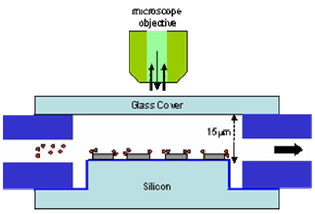

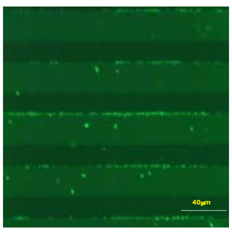

Virus Size ~ 250x350nm
Picture taken at: 10Vpp, 1MHz, DI water ~1.5μS/cm, flow rate ~0.1μl/min

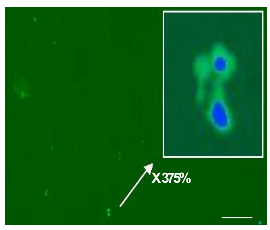

400x magnification: viral surface lipid membrane labeled green (DiOC63) and viral nucleic acids were stained blue (Hoechst 33342 stain)

D. Akin, H. Li, R. Bashir, *Nano Letters*, 4, pp. 257 -259, 2004

22

PURDUE UNIVERSITY

Release voltage vs. diameter for particle collecting the electrode edge, considering the Brownian motion

Polarization factor=0.5,

flow rate 0.1μm/min, in the channel with cross-section 350x11.6μm2,

interdigitated electrodes with 23μm width and17μm spacing

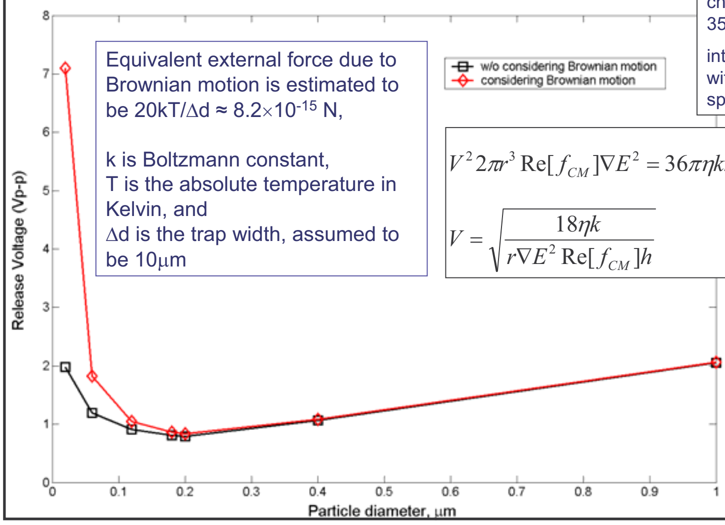

Equivalent external force due to Brownian motion is estimated to be $20kT/\Delta d \approx 8.2\times10^{-15}$ N,

k is Boltzmann constant,
T is the absolute temperature in Kelvin, and
Δd is the trap width, assumed to be 10μm

$$V^2 2\pi r^3 \,\mathrm{Re}[f_{CM}]\nabla E^2 = 36\pi\eta k r\left(\frac{r}{h}-\frac{r^2}{h^2}\right) \approx 36\pi\eta k\frac{r^2}{h}$$

$$V=\sqrt{\frac{18\eta k}{r\nabla E^2\,\mathrm{Re}[f_{CM}]h}}$$

PURDUE UNIVERSITY

Micro-fluidic Characterization

- Micro-Particle Imaging Velocimetry (μPIV)

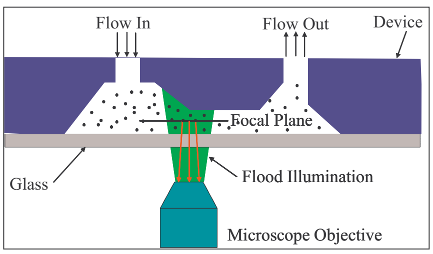

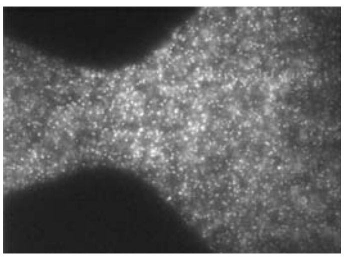

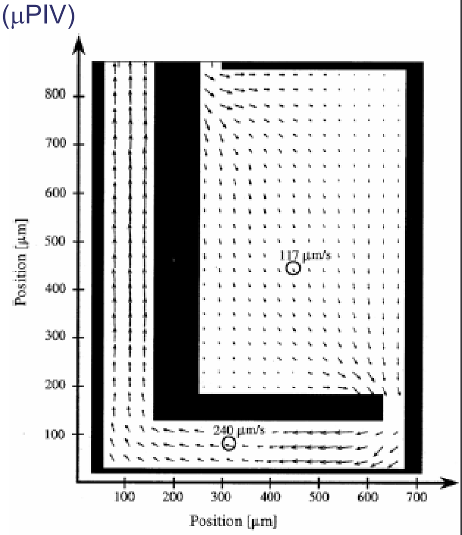

Wereley, et al. Purdue

Gomez, et al. 2001

PURDUE UNIVERSITY

Key Topics

- Biochips/Biosensors and Device Fabrication
- Cells, DNA, Proteins
- Micro-fluidics
- **Biochip Sensors & Detection Methods**
- Micro-arrays
- Lab-on-a-chip Devices

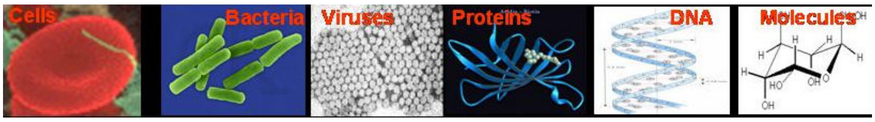

25

PURDUE UNIVERSITY

Biochip Sensors

- Detect cells (mammalian, plant, etc.), microorganisms (bacteria, etc.), viruses, proteins, DNA, small molecules
- Use optical, electrical, mechanical approaches at the micro and nanoscale in biochip sensors

26

PURDUE UNIVERSITY

Sensing Methods in BioChips

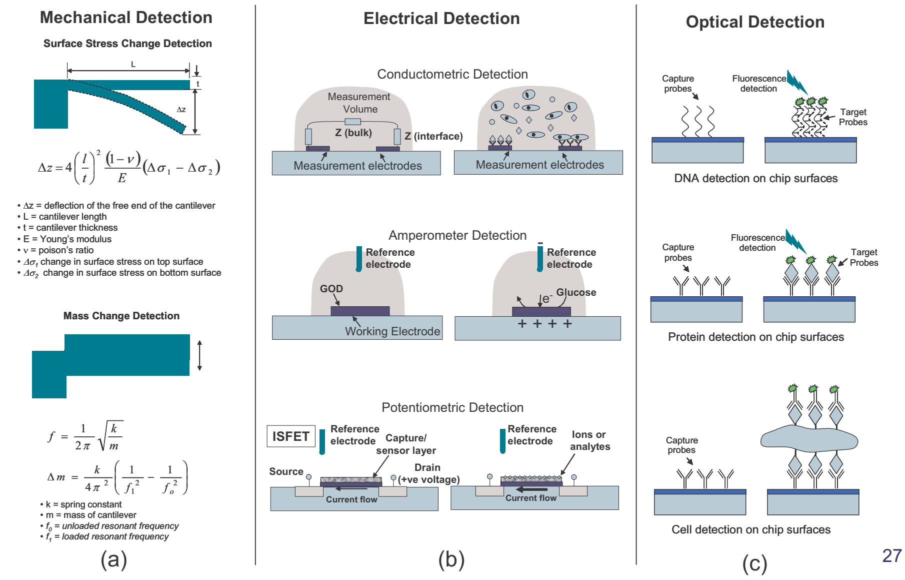

27

PURDUE UNIVERSITY

1. Microcantilever Stress Sensors

Mechanical Detection

Surface Stress Change Detection

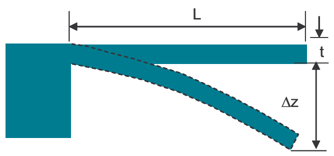

$$\Delta z = 4\left(\frac{l}{t}\right)^2 \frac{(1-\nu)}{E}(\Delta\sigma_1 - \Delta\sigma_2)$$

- Δz = deflection of the free end of the cantilever
- L = cantilever length
- t = cantilever thickness
- E = Young's modulus
- ν = poison's ratio
- $\Delta\sigma_1$ change in surface stress on top surface
- $\Delta\sigma_2$ change in surface stress on bottom surface

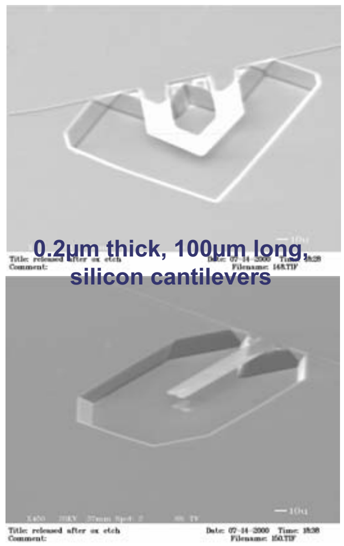

0.2µm thick, 100µm long, silicon cantilevers

28

PURDUE UNIVERSITY

Microcantilever Stress Sensors

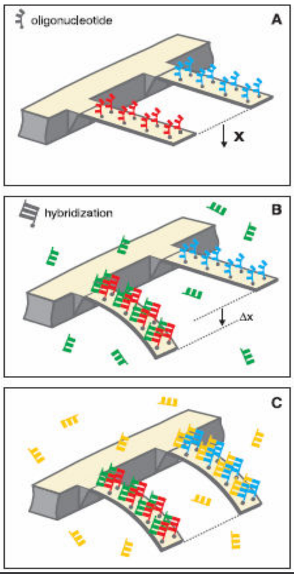

IBM Zurich Research:
DNA Detection

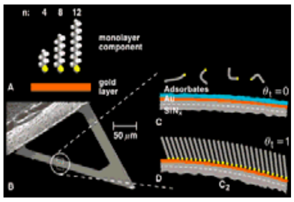

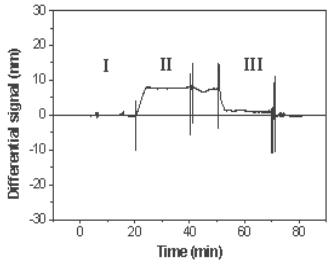

Fritz et al, *Science*, **288,** April 2000

PURDUE UNIVERSITY

Microcantilever Stress Sensors

Detection of PSA,
Prostate Specific Antigen
(cancer marker protein in blood)

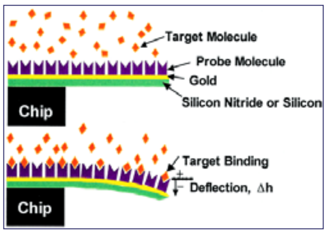

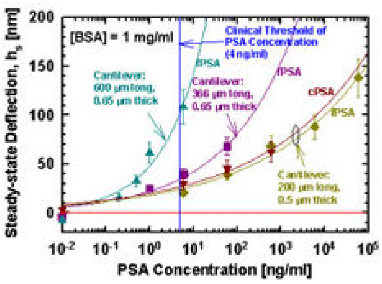

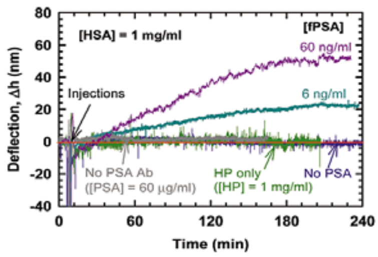

- PSA ~ 30kDa ~ 30 x 1e3 x 1.66e-24gm
- In 1ng/ml ~ 2e10 molecules/ml
- Area of 20um x 60um, each protein 10nm x 10nm → ~1e8 proteins

Wu et al, Nature Biotechnology, **19,** September 2001

Deflections have been measured with a resolution of **0.4x10-12 m.***

PURDUE
UNIVERSITY

Polymer/Silicon Cantilever Sensors

- **Environmentally sensitive micro-patterned polymer structures on cantilevers**
- **Hydrogel patterned on cantilever and then exposed to varying pH**

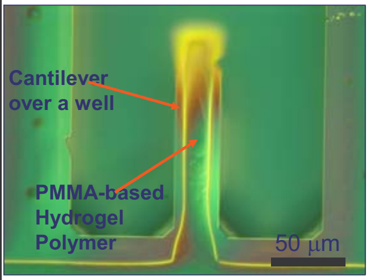

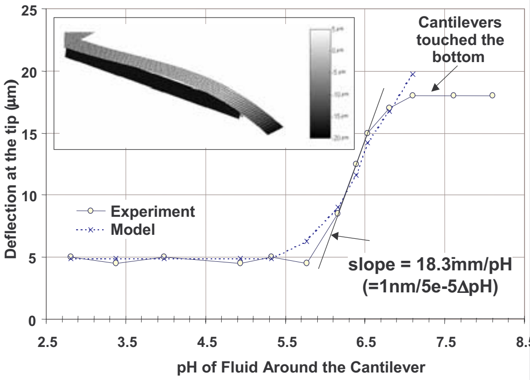

- ΔpH = 1-10e-5
- pH = 6.5 → ~ 1.9e5 H^+ in 1000µm^3
- ΔpH = 5e-4 → change of ~ 150 H^+

R. Bashir, J.Z. Hilt, A. Gupta, O. Elibol, and N.A. Peppas, Applied Physics Letters, Oct 14th, 2002;
J. Zachary Hilt, Amit K. Gupta, Rashid Bashir, Nicholas A. Peppas Biomedical Microdevices, September 2003, Volume 5, Issue 3, 177-184

PURDUE
UNIVERSITY

2. Microcantilever Mass Sensors

Unloaded Resonant Frequency :

$$f_0 = \frac{1}{2\pi}\sqrt{\frac{k}{m^*}}$$

Spring constant for a rectangular shaped cantilever beam: $k = \frac{Et^3 w}{4l^3}$

Loaded Resonant frequency : $f_1 = \frac{1}{2\pi}\sqrt{\frac{k}{m^* + \delta m}}$

δm is the added mass

$$\Delta m = \frac{k}{4\pi^2}\left(\frac{1}{f_1^2} - \frac{1}{f_o^2}\right)$$

- k = spring constant
- m = mass of cantilever
- *f_0 = unloaded resonant frequency*
- *f_1 = loaded resonant frequency*

Mass Change Detection

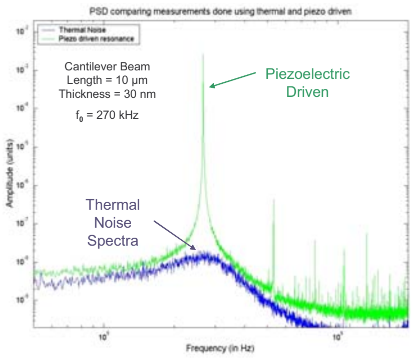

PURDUE UNIVERSITY

Detection of Bacterial Mass

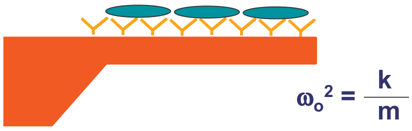

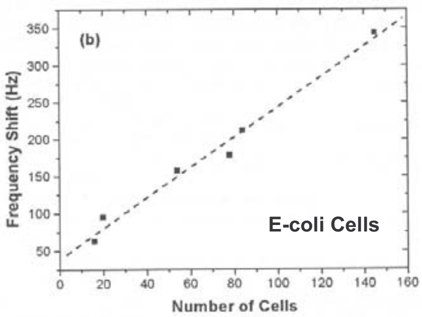

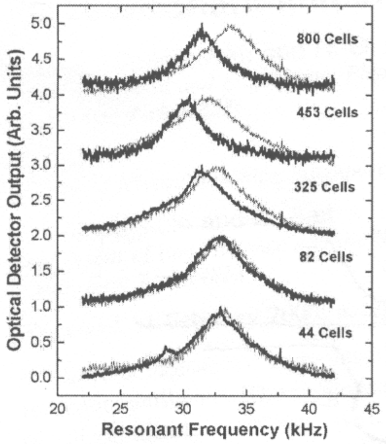

Craighead, et al. APL, 77, 3, 17th July 2001, 450-452

33

PURDUE UNIVERSITY

Detection of Listeria Cell Mass

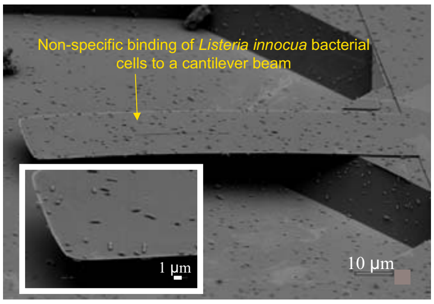

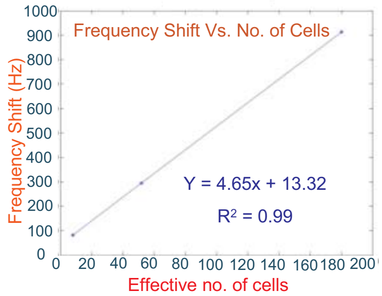

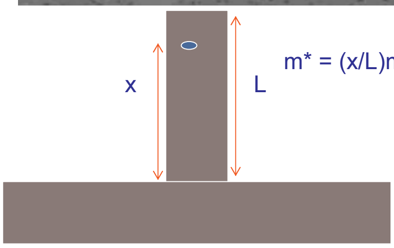

$m^* = (x/L)m$

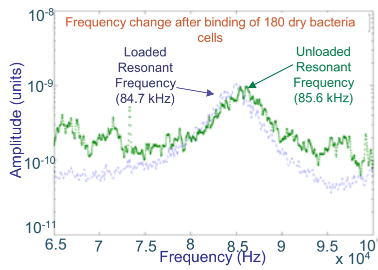

A. Gupta, D. Akin, R. Bashir, SPIE, 2003.

34

PURDUE UNIVERSITY

Minimum Detectable Mass

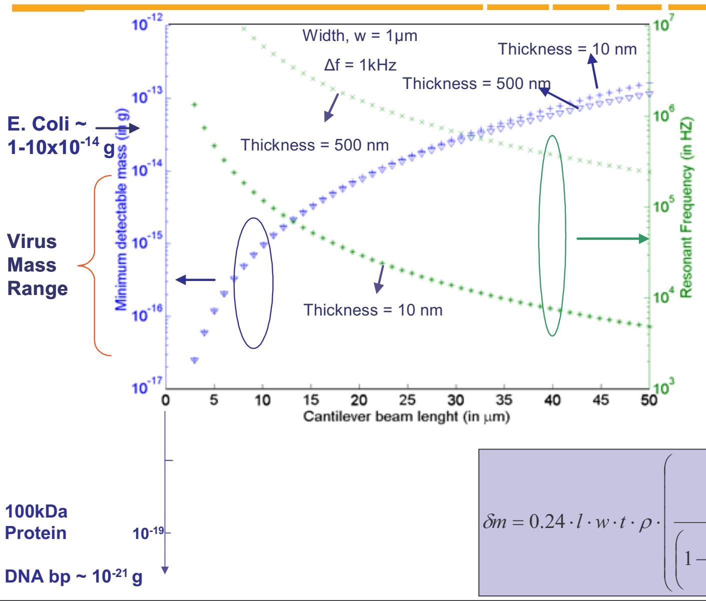

$$\delta m = 0.24 \cdot l \cdot w \cdot t \cdot \rho \cdot \left(\frac{1}{\left(1 - \frac{2\pi\delta f (0.98) l^2}{t}\sqrt{\frac{\rho}{E}}\right)^2} - 1 \right)$$

PURDUE UNIVERSITY

Minimum Detectable Mass

- The frequency measurement is limited by thermo-mechanical noise on the cantilever beam.
- Minimum Detectable Frequency, Δf,min = $\frac{1}{A}\sqrt{\frac{f_0 k_B TB}{2\pi kQ}}$
- Minimum Detectable Mass, Δm,min = $\frac{1}{A}\sqrt{\frac{4 k_B TB}{Q}} \frac{m_{eff}^{5/4}}{k^{3/4}}$
- k_B = Boltzmann constant
- T = Temperature in Kelvin
- B = Bandwidth measurement, (~ 1 kHz)
- Q can increase by 100X by driving the cantilevers

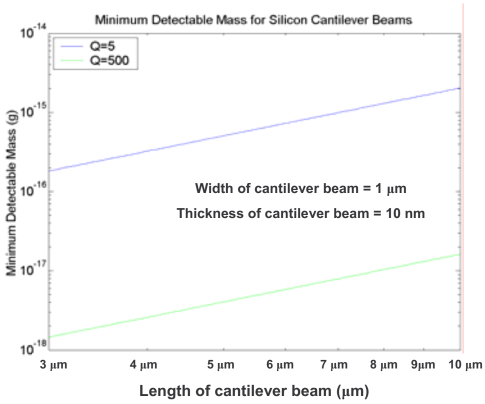

36

PURDUE UNIVERSITY

Fabrication Process Flow

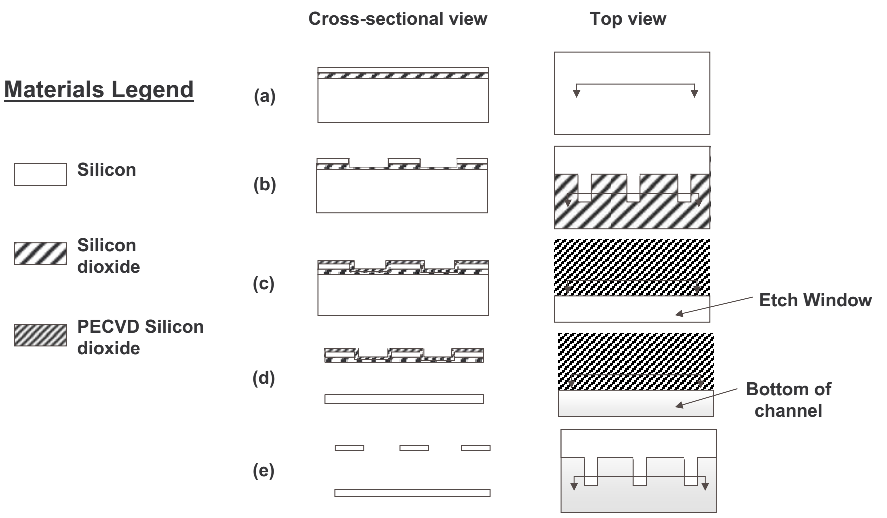

37

PURDUE UNIVERSITY

SEM Pictures of Cantilevers

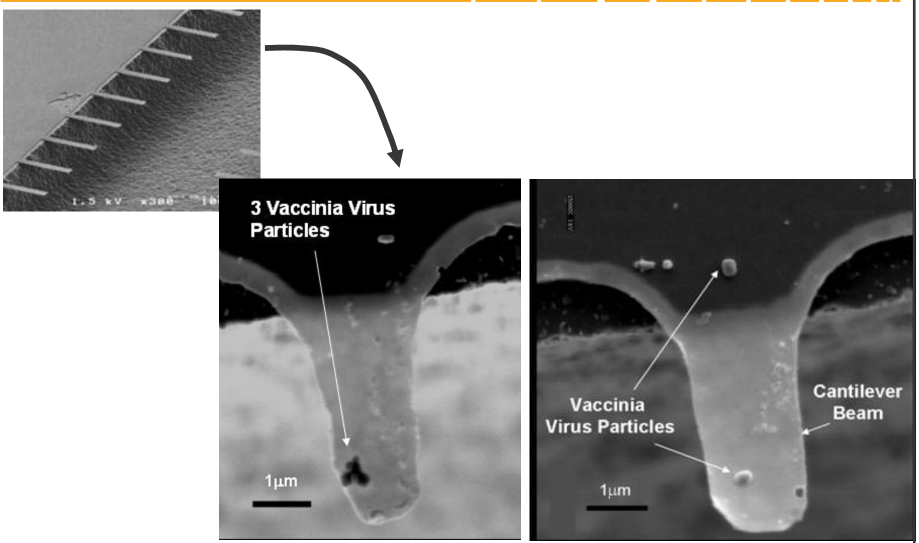

A. Gupta, D. Akin, R. Bashir, *Applied Physics Letters*, March 15, 2004.

38

Frequency Shift vs. No. of Particles

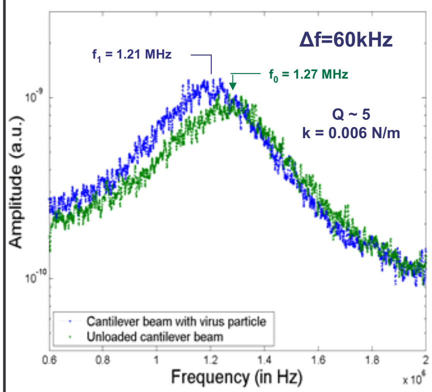

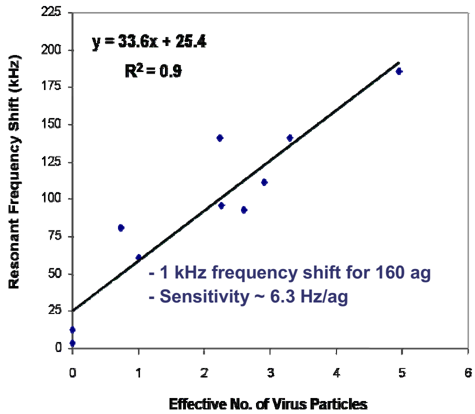

- Average mass of Vaccinia Virus ~ 9.5fg
- Work on going to integrated concentration elements
- Integrated Abs on cantilevers

A. Gupta, D. Akin, R. Bashir, *Applied Physics Letters*, March 15, 2004.

Mass of Molecules

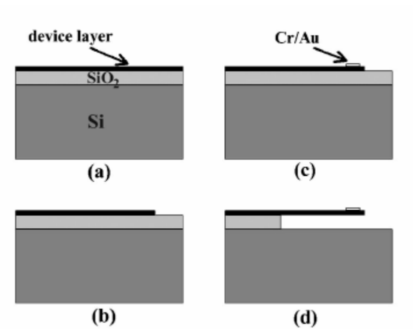

To probe the amount of thiolate binding to the Au contacts, we have measured the frequency spectra before and after the thiolate self-assembly. Figure 14 shows the measured shift in the resonant frequency for DNP-PEG4-C11thiol binding on 50- and 400-nm-diam Au contacts. The measured frequency shifts were 125 Hz and 1.10 kHz, corresponding to calculated masses of 6.3 and 213.1 ag, respectively.

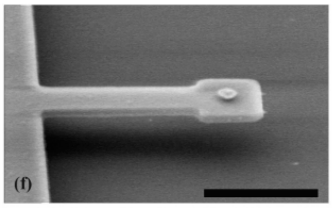

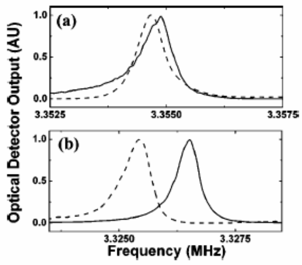

FIG. 14. Experimentally measured frequency spectra before (solid line) and after (dashed line) the adsorption of the thiolate on (a) 50- and (b) 400-nm-diam Au contact. Rectangular beam dimensions were $l = 10\ \mu m$, $w = 1\ \mu m$, and $t = 250$ nm.

Ilic, B., Craighead, H.G.; Krylov, S.; Senaratne, W.; Ober, C.; Neuzil, P.
Source: Journal of Applied Physics, v 95, n 7, 1 April 2004, p 3694-703

PURDUE UNIVERSITY

Electrical/Electrochemical Detection

1. amperometric biochips, which involves the electric current associated with the electrons involved in redox processes,
2. potentiometric biochips, which measure a change in potential at electrodes due to ions or chemical reactions at an electrode (such as an ion Sensitive FET), and
3. conductometric biochips, which measure conductance changes associated with changes in the overall ionic medium between the two electrodes.

41

PURDUE UNIVERSITY

1. Amperometric Detection

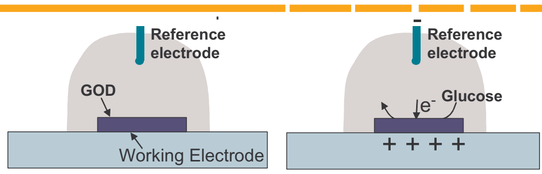

β-D-Glucose + O_2 + H_2O —(Glucose Oxidase)→ D-gluconic acid + H_2O_2

hydrogen peroxide is reduced at -600mV at Ag/AgCl anode reference electrode.

- Detection of Glucose, Lactate, Urea, etc.
- Enzyme entrapped in a gel
- Surface regeneration and sensor reusability

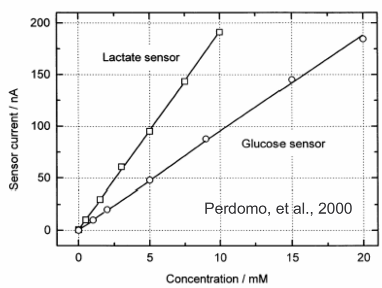

42

Detection of DNA Hybridization

- Capture probes are attached to electrodes.
- Target DNA binds to complementary probes
- DNA sequences, called signaling probes, with electronic labels attach to them (ferrocene-modified DNA oligonucleotides, E1/2 of 0.120 V vs. Ag/AgCl, act as signaling probes).
- Binding of the target sequence to both the capture probe and the signaling probe connects the electronic labels to the surface.
- The labels transfer electrons to the electrode surface, producing a characteristic signal.

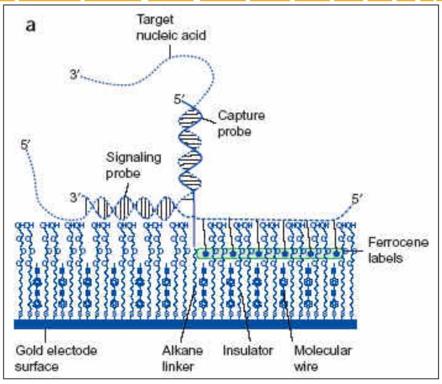

Umek, et al. J. Molecular Diagnostics, 3, 74-84, 2001
Drummond, Hill, Barton, Nature Biotech, v21, n10, Oct 2003, p1192
http://www.motorola.com/lifesciences/esensor/tech_bioelectronics.html

2. Potentiometric Sensors

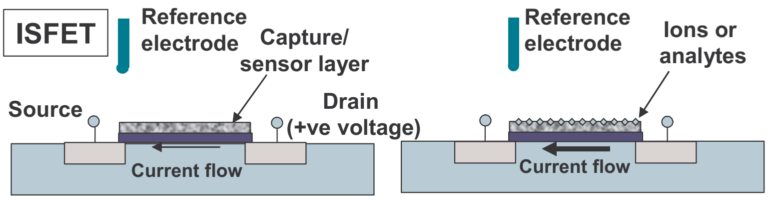

- ISFETs, ChemFETs, etc.
- Potential difference between the gate and the reference electrode in the solution
- Change in potential converted to a change in current by a FET or to a change in capacitance in low doped silicon
- Gate material is sensitive to specific targets
- pH, Ions, Charges

Nanoscale pH Sensors

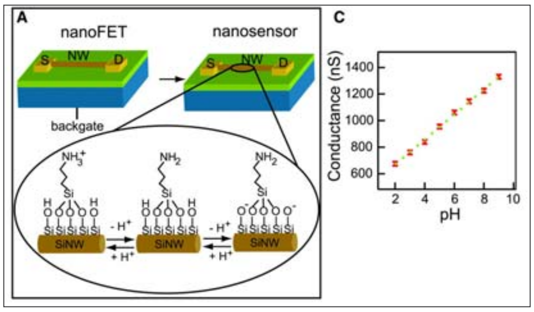

- Label Free !!
- Detection of pH change
- Detection of protein binding

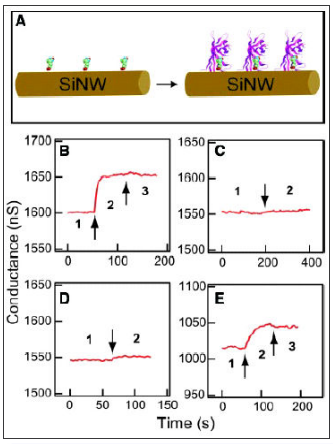

- Streptavidin binding detection down to at least 10 pM.
- Substantially lower than the nanomolar range demonstrated by other procedures.

Y. Cui, Q. Wei, H. Park, and C.M. Lieber. Nanowire nanosensors for highly sensitive and selective detection of biological and chemical species. *Science*, 293:1289–1292, 2001.

45

Integrated Silicon Nanowire Sensors

Objectives:

- Bio-sensors with electronic output
- Capability of dense arrays integrated with ULSI silicon
- Direct Label Free Detection of DNA and Proteins

- Plate Size ~ 20nm X 1μm X 3μm
- Wire Size ~ 20nm X 20nm X 3μm

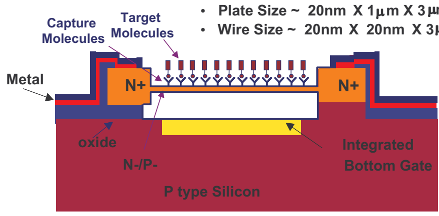

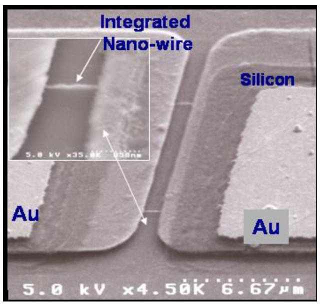

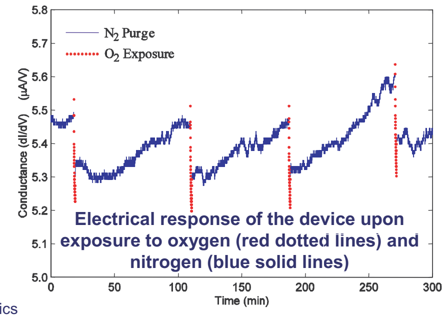

O. H. Elibol, D. Morisette, D. Akin, R. Bashir, Applied Physics Letters. Volume 83, Issue 22, pp. 4613-4615, December 1, 2003

46

Field Effect Sensing of DNA

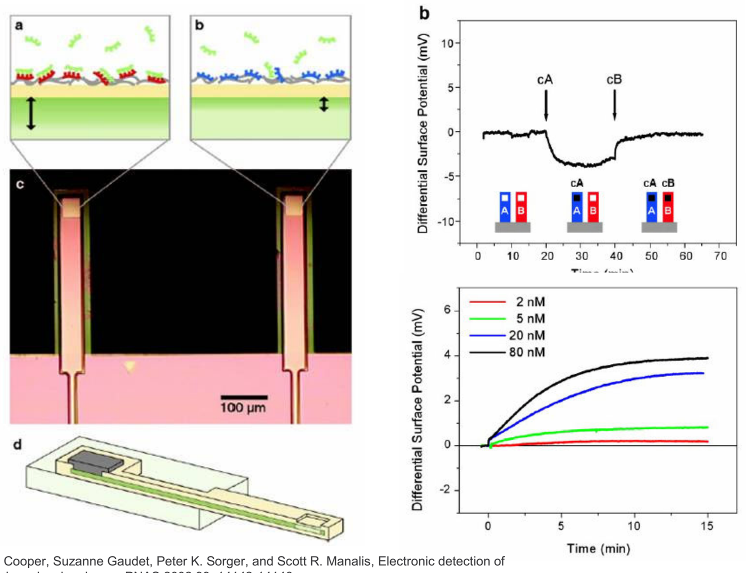

J. Fritz, Emily B. Cooper, Suzanne Gaudet, Peter K. Sorger, and Scott R. Manalis, Electronic detection of DNA by its intrinsic molecular charge, PNAS 2002 99: 14142-14146.

3. Conductometric Biochips

- Conductometric sensors measure the changes in the electrical impedance between two electrodes, where the changes can be at an interface or in the bulk region and can be used to indicate biomolecular reaction between DNA, Proteins, and antigen/antibody reaction, or excretion of cellular metabolic products.

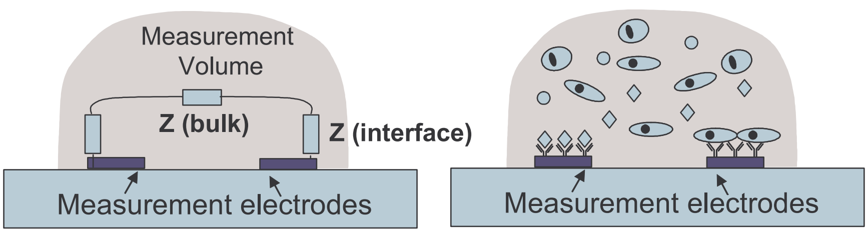

PURDUE
UNIVERSITY

Nanoparticle Mediated DNA Detection

- Au nanoparticles assemble between two electrodes if DNA is hybridized
- Silver staining of the Au nanoparticles
- Conductance changes between micro-scale electrodes indicate DNA hybridization
- Sensitivity of $5x10^{-13}$ M shown

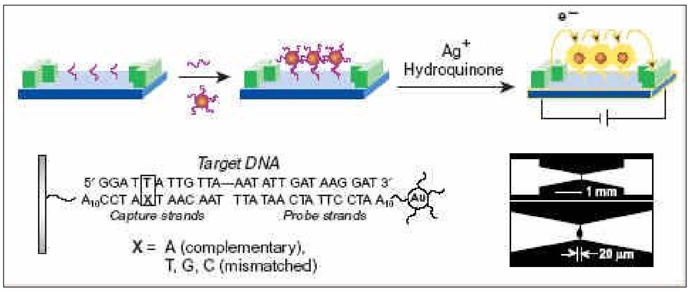

Park, S.-J.; Taton, T. A.; Mirkin, C. A. Array-Based Electrical Detection of DNA Using Nanoparticle Probes, Science, 2002, 295, 1503-1506.

PURDUE
UNIVERSITY

Micro-fluidic Devices for Conductance Detection of Bacterial Metabolism

- Detection of Cell Growth by measuring their metabolic activity in micro-fluidic devices

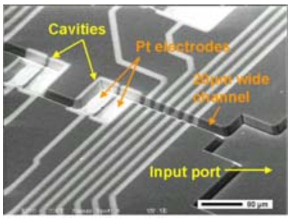

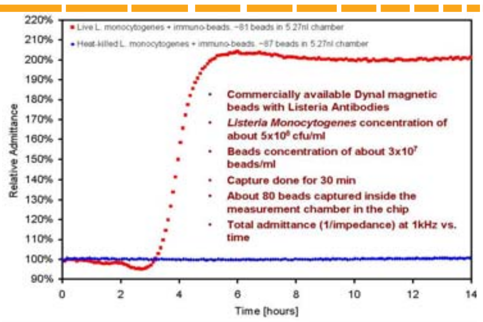

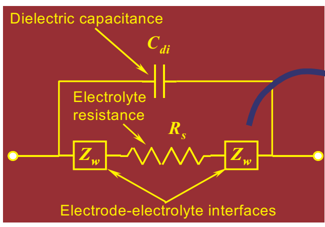

Electrode-Electrolyte Interface Model:

$$Z_w = \frac{1}{(j\omega)^n B}$$

Constant-angle impedance

R. Gomez, et al., Biomedical Micro-Devices, vol. 3, no. 3, p. 201-209, 2001.
R. Gomez, et al., Sensors and Actuators, B, 86, 198-208, 2002.

4. Cell-Based Sensors/Biochips

- The transductions of the cell sensor signals maybe achieved by:
  - the measurement of transmembrane and cellular potentials,
  - impedance changes,
  - metabolic activity,
  - analyte inducible emission of genetically engineered reporter signals, and
  - optically by means of fluorescence or luminescence.

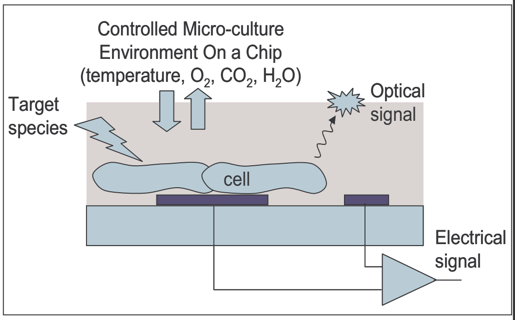

L. Bousse, Whole cell biosensors, Sensors and Actuators B (Chemical), Vol. B34, No. 1-3, August 1996, pp. 270-5.
J.J. Pancrazio, J.P. Whelan, D.A. Borkholder, W. Ma, D.A. Stenger, Development and application of cell-based biosensors, Annals of Biomedical Engineering, Vol. 27, No. 6, November 1999, pp. 697-711.
D.A. Stenger, G.W. Gross, E.W. Keefer, K.M. Shaffer, J.D, Andreadis, W. Ma, J.J. Pancrazio, Detection of physiologically active compounds using cell-based biosensors, Trends in Biotechnology, Vol. 19, No. 8, August 1, 2001, pp. 304-309.

5. Micro/Nano-scale Coulter Counter

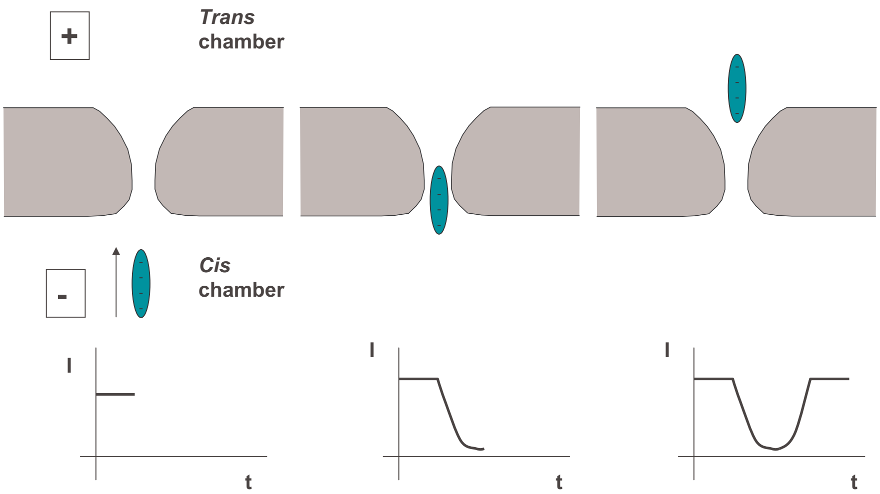

PURDUE
UNIVERSITY

Micro-pore for cellular studies

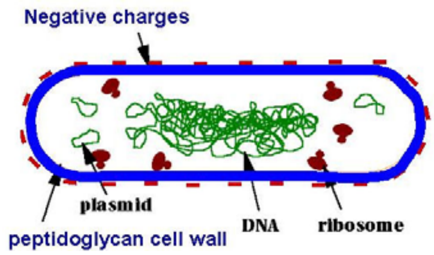

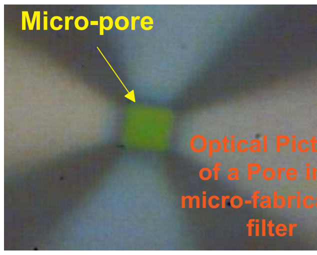

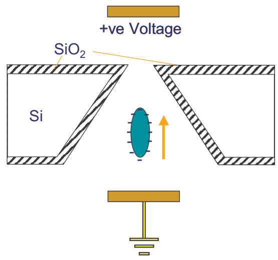

Cross section of micro-fabricated pore

- Micro-devices for single cell characterization – utilize the charge properties
- Micro-fabricate a pore where single entity can pass

PURDUE
UNIVERSITY

Microscale Coulter Counter

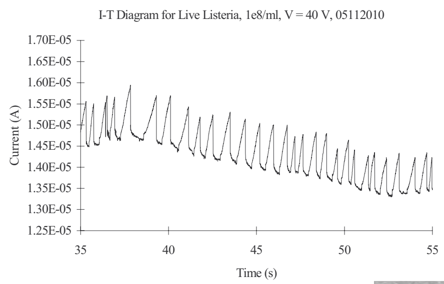

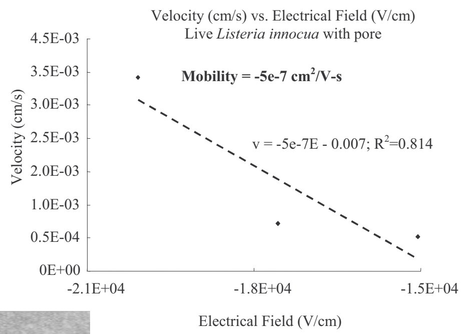

Live *Listeria innocua* with a well-defined cell wall

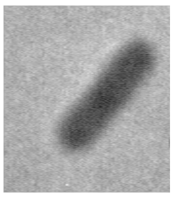

H. Chang, A. Ikram, T. Geng, F. Kosari, G. Vasmatzis, A. Bhunia, and R. Bashir, "Electrical characterization of microorganisms using microfabricated devices", Journal of Vacuum Society and Technology B, 20, 2058 (2002).

PURDUE UNIVERSITY

Nanoscale DNA Coulter Counter

- α-hemolysin channel, a biological protein based-pore, was utilized.
- Pore size is 2.6 nm.
- Both RNA and DNA molecules were observed traversing the nanochannel.

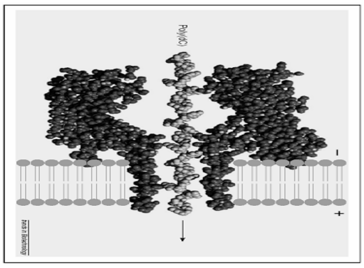

α-hemolysin nanochannel

The model of DNA passing through an α-hemolysin channel.

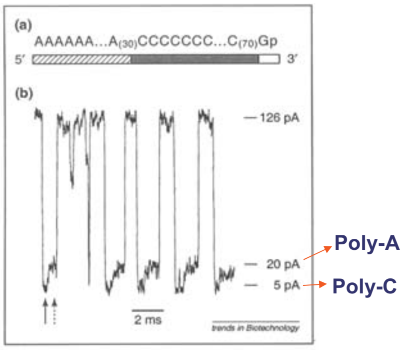

Kasianowicz et al., 1996, Meller, et. al. 2000.

55

PURDUE UNIVERSITY

Fabrication Techniques

- Solid-state based nanopore. Made in silicon nitride membrane.
- Pore size: 3 nm and 10 nm.
- The relation among DNA lengths and translocation times and applied biases were determined.

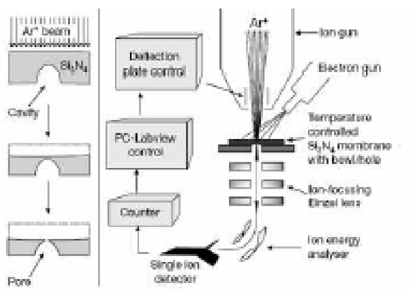

The fabrication of Li's nanopore. From *Li et. al. Nature, 2001.*

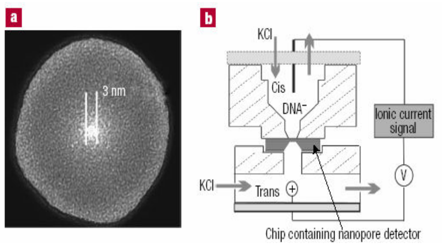

TEM of Li's nanopore. b. DNA measurement setup in Li's work. From *Li et. al. Nature Materials, 2003*

56

PURDUE
UNIVERSITY

DNA Translocation

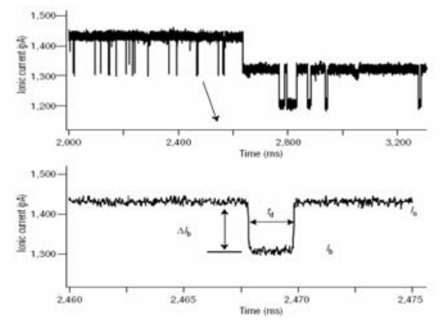

Current fluctuations when DNA was passing through the pore

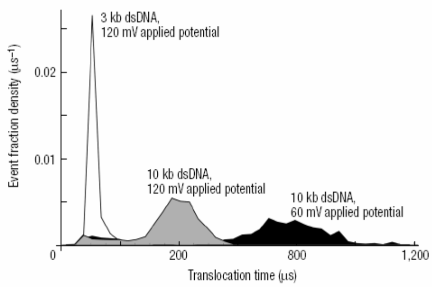

Histograms of relation among DNA lengths, translocation times and applied biases.

Li et. al. 2003

57

PURDUE
UNIVERSITY

Silicon Based Nanopore

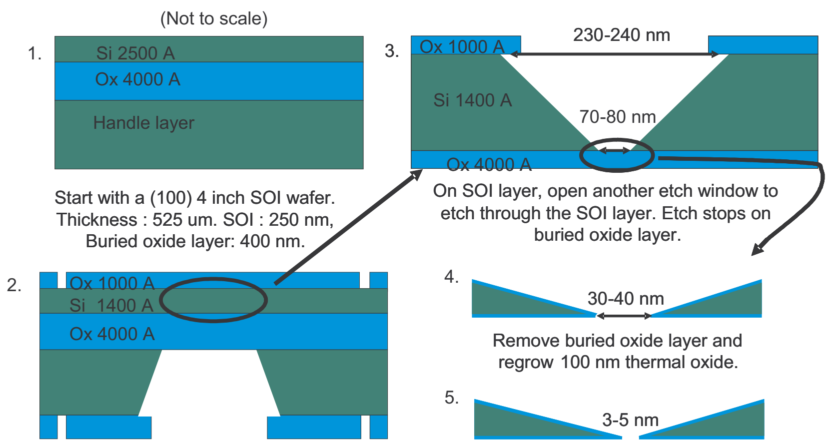

Grow thermal oxide on wafer surface and open etch window to etch through the handle layer. Etch stops on buried oxide layer.

Shrink the pore to 3 –5 nm by TEM

58

Pore shrinking and shape changing (After Thermal Oxidation, Oxide Thickness = 50 nm)

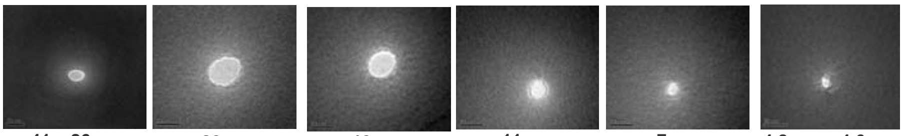

41 x 26 nm (300,000 X)	23 nm (1,000,000 X)	19 nm (1,000,000 X)	11 nm (1,000,000 X)	7 nm (1,000,000 X)	4.2 nm x 4.6 nm 1,000,000 X)

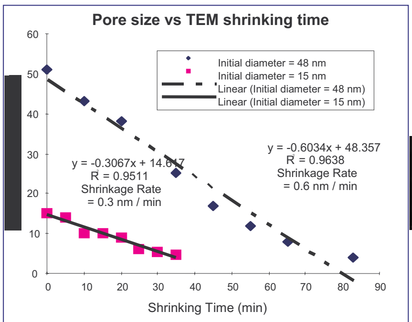

Slopes in the plot are the shrinkage rates. Different initial pore size had different shrinkage rates.

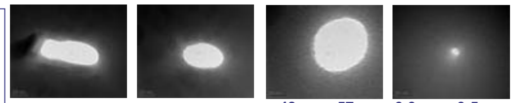

9nm x 198nm Initial pore | 80nm x 156nm 90 min | 48nm x 57nm 250 min | 3.3nm x 3.5nm 334 min

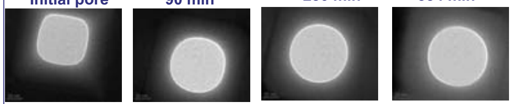

168nm x 172nm | 187nm x 189nm 20 min | 200nm x 201nm 45 min | 206 nm x 208 nm 58 min

A. J. Storm, J.H. Chen, X.S. Ling, H.W. Zanderbergen and C. Dekker, "Fabrication of solid-state nanopores with single-nanometre precision", Nature Materials, 2, 537 (2003).

H. Chang, F. Kosari, G. Andreadakis, G. Vasmatzis, E. Basgall, A. H. King, and R. Bashir, "Towards Integrated Micro-Machined Silicon-Based Nanopores For Characterization Of DNA", Hilton Head MEMS conference, 2004, Hilton Head, South Carolina.

59

Explanation – Minimization of Surface Energy

From *Storm et. al. 2003*

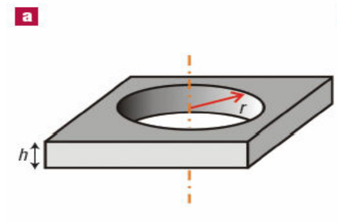

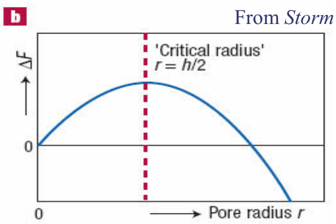

Surface free energy:

$\Delta F = \gamma \Delta A = 2\pi\gamma(rh - r^2)$

where γ is the surface tension of the fluid,

ΔA is the change in surface area.

r is the radius of the pore right after the final oxidation,

h is oxide thickness.

The shrinkage/expanding of pores with different radii and oxide thicknesses.

Sample name Shrinkage/Expansion (S/E)	Average radius of the pore r (nm)	Grown oxide thickness d (nm)	The ratio of r/d
103003_4 S	9	79	0.11
102503_4 S	38	100	0.38
110603_2 S	51.5	130	0.40
[illegible] E	82	90	0.91
[illegible] E	138	120	1.15
[illegible] E	110	54	2.04

H. Chang, F. Kosari, G. Andreadakis, G. Vasmatzis, E. Basgall, A. H. King, and R. Bashir, "Towards Integrated Micro-Machined Silicon-Based Nanopores For Characterization Of DNA", Hilton Head MEMS conference, 2004, Hilton Head, South Carolina.

60

Integrated Optical Detection

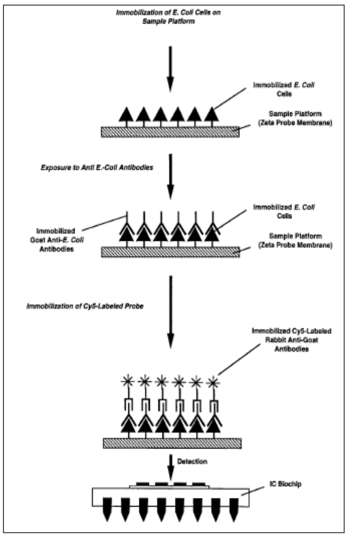

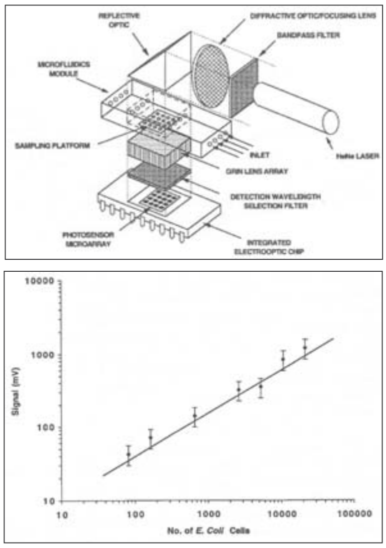

Stokes, Griffen, Vo-Dinh, Fresenius J Anal Chem, 369,:295-301, 2001